Available online www.ejaet.com

European Journal of Advances in Engineering and Technology, 2018, 5(1): 1-7

Research Article ISSN: 2394 - 658X

Laser Additive Manufacturing: Static Properties and Microstructure Characterization of a Near-Eutectic Aluminium Alloy

K.V. Sudhakar, Bryce Abstetar, Ronda Coguill, Scott Coguill, Taylor Winsor and Bruce Madigan

Montana Tech of the University of Montana, Butte, MT 59701, USA
kvsudhakar@mtech.edu

ABSTRACT

Static properties, microstructure and fracture morphologies of a near-eutectic aluminium alloy produced by a laser additive manufacturing (LAM) method were investigated. Laser powder bed fusion process was used to 3D-print tensile test specimens at 0, 30, 60 and 90-degree build angle orientations, with known processing parameters. Tensile tests were conducted on MTS Landmark servo hydraulic Test System. Optical microscope (Leica DM750P with Leica application suite software) was used to determine the microstructures. SEM-LEO 1430 VP model was utilized to investigate the fracture surface features. Similarities and differences were present in the test results for mechanical properties. Namely, ultimate tensile strength, and elastic modulus for the LAM samples were found to be on par with that of a wrought aluminium alloy. In contrast, there was a distinct difference in yield for the wrought versus LAM. There were also differences in percent elongation as a function of build orientation and LAM versus wrought specimens. Distinct microstructures were observed that consisted of ripples, pores, voids, and cellular structure. Fracture characteristics demonstrated dimple fracture surface features demonstrating a good level of toughness.

Keywords*:* Near eutectic aluminium alloy, laser additive manufacturing, tensile properties, microstructure, fracture

---

INTRODUCTION

Laser additive manufacturing (LAM) is one of the latest innovative manufacturing technologies used to produce near net/net shaped industrial products [1]. LAM has been used for the last several years and is now widely used for various materials [2-6]. LAM is also called 3D-printing that is used for the rapid manufacturing of metal alloy components. In the recent past, there has been an increasing number of investigations on LAM of near eutectic Al-alloys because of their use as lightweight structures with complex geometries [7-9]. Near eutectic aluminium alloy (AlSi10Mg) is a traditional cast alloy that is typically produced by die-casting. This alloy has been extensively used in the aircraft, aerospace, and automotive industries due to their very good combination of mechanical properties. It has good weldability because of its near eutectic composition of aluminium and silicon. Its age hardening effect is enhanced by the addition of magnesium element. There are quite a few literatures specifically discussing the effect of microstructure on processing parameters of SLM-fabricated near eutectic aluminium alloy [10-12]. A few of the recent literatures specific to the Aluminium based alloys are discussed [13-17].

Earlier work [18-22] focused mainly on experimental device design and fabrication parameter optimization. There has been limited work regarding the mechanical performance and fracture behaviour of as-deposited/as-built components [23]. The authors of the present investigation have presented a technical paper on an additively manufactured 316L stainless steel in a recent conference [24].

The objective of the present investigation is to evaluate tensile properties, microstructure, and fracture morphologies of a near eutectic aluminium alloy, as a function of material build angle orientation, produced by laser additive manufacturing process. Also, the results of the LAM produced specimens are compared with that of the wrought aluminium alloy.

MATERIALS AND METHODS

Material and LAM Processing

The material used is near eutectic aluminium alloy with the following composition (wt. %); Si: 10%, Mg: 0.25%, Al: balance. LAM processing parameters used in this investigation are; Hatch spacing: 0.19 mm; Laser power: 350 W; Laser scan speed: 1150 mm/s; and Energy density: 1.6 J/mm^2. Figure 1 (a) shows the build direction and the sectioning orientation of the specimen and (b) reveals the build angle orientations of the test specimens at 0^0, 30^0, 60^0, and 90^0.

Tensile Test

Tensile test was performed using an MTS Landmark servo hydraulic Test System that determines the material's tensile properties by producing a stress-strain curve. The diameter of the reduced section was 8.9 mm and the gage length was 35.6 mm. The tests were carried out as per the ASTM E8/E8M standard. Tensile properties, namely; elastic modulus, yield strength, and tensile strength were evaluated.

Microstructure Characterization

Microstructures of near eutectic Aluminium alloy were investigated using Leica DM750P optical microscope with Leica application suite software. The samples were etched using Keller's reagent (95 ml distilled water, 2.5 ml HNO_3, 1.5 ml HCl, 1.0 ml HF).

Investigation of Fracture Modes

Both LAM and wrought samples were examined using a LEO 1430VP scanning electron microscope.

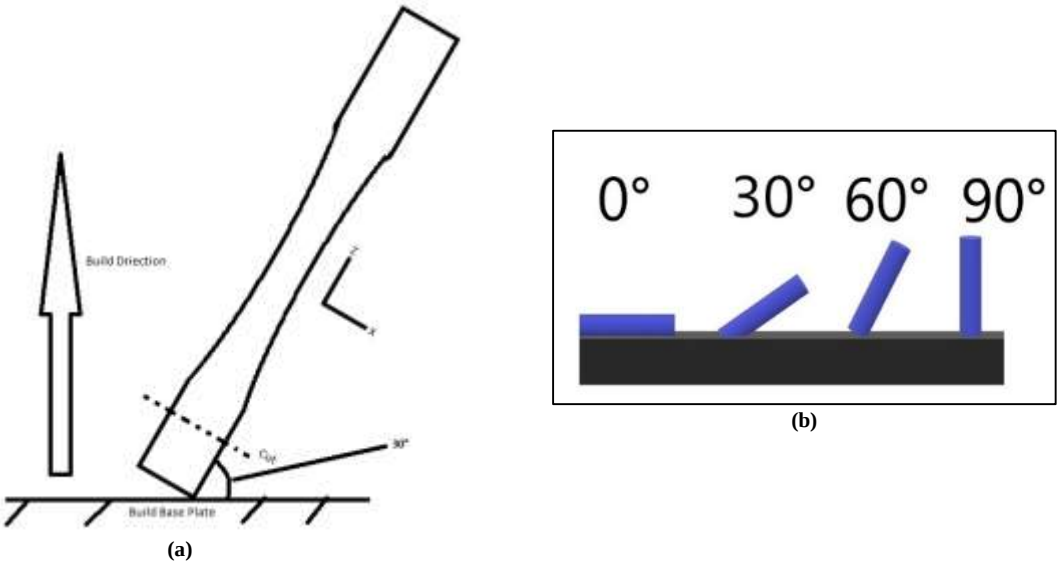

(a) **(b)**

Fig. 1(a) Build Direction and Sectioning Orientation, (b) Build angle in relation to build plate

RESULTS AND DISCUSSION

Stress-Strain Behaviour

The stress-strain behaviour of the wrought and near-eutectic additive manufactured aluminium alloy is presented in Figure 2. All the specimens were tested at a strain rate of 10^{-2} per second. The mechanical properties of additively manufactured aluminium alloy, with the exception of yield strength and % elongation, were on-par with that of the wrought alloy.

Influence of Specimen Build Angles on Elastic Modulus

The average elastic modulus of wrought and LAM processed samples are presented in Figure 3 and they are determined to be almost the same. The specimen build angles do not seem to have any effect on the elastic modulus of the additively manufactured aluminium alloy.

Influence of Specimen Build angle on Yield Strength

Figure 4 shows the variation of average yield strength with different specimen orientations and they are observed to be almost on par with each other only for the 3D printed specimens. Again, the specimen build angles have no effect on the yield strength of near-eutectic aluminium alloy printed specimens. But, as seen in the Figure 1, individual specimen stress-strain results, the wrought specimens did not yield in the same manner.

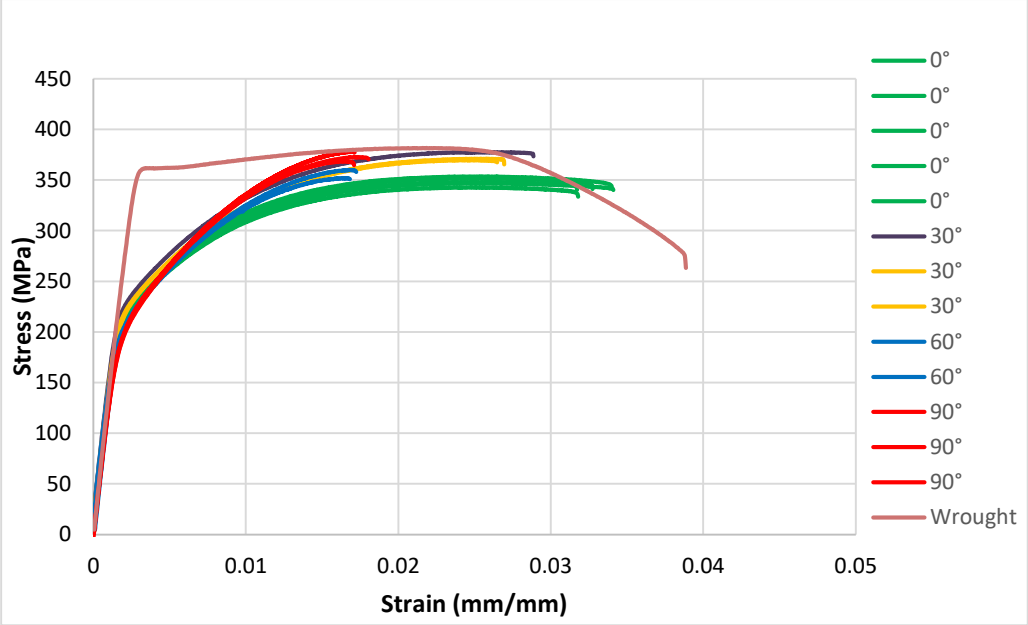

Fig. 2 Stress-strain behaviour of a near-eutectic and wrought aluminium alloy

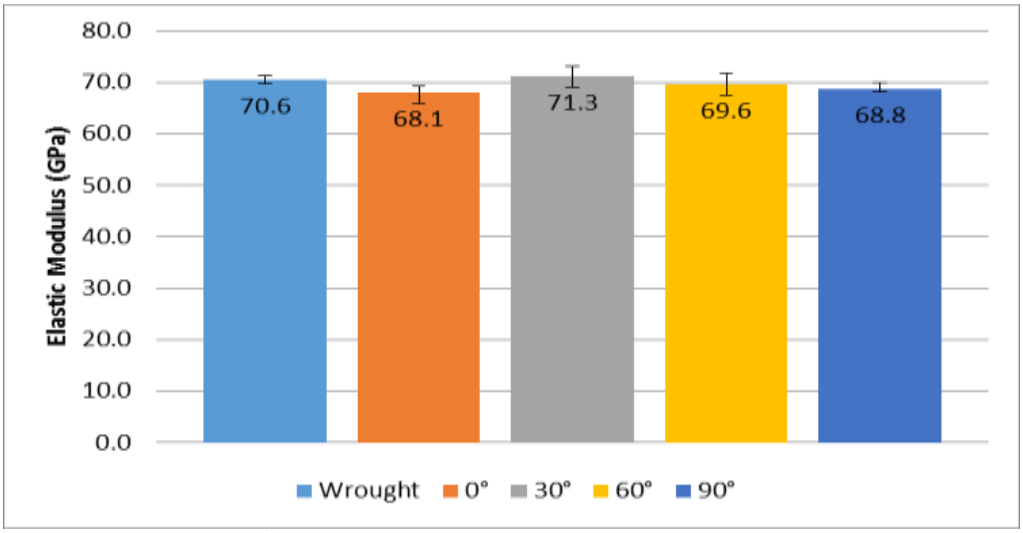

Fig. 3 Average elastic modulus for SLM and wrought tensile specimens (error bars represent one standard deviation)

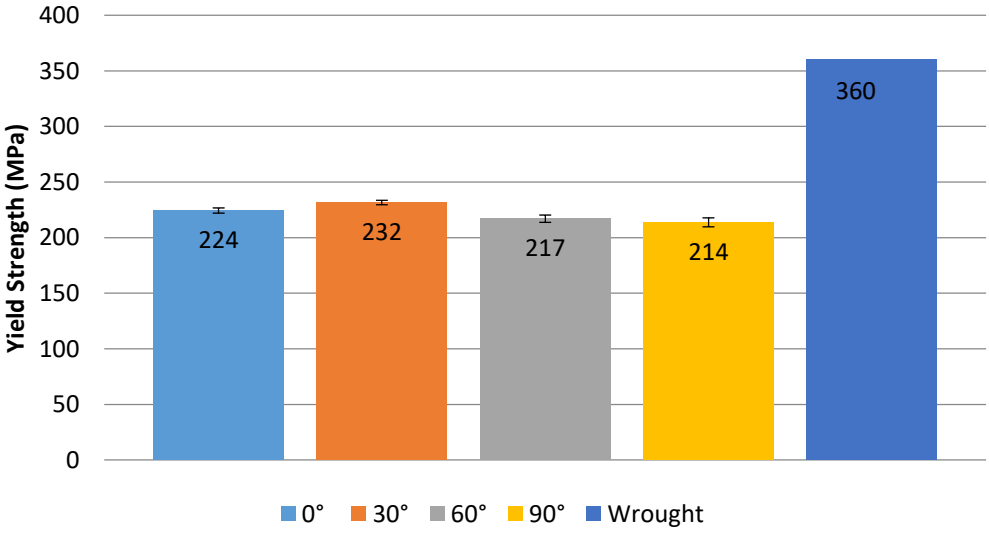

Fig. 4 Variation of yield strength with specimen build orientation

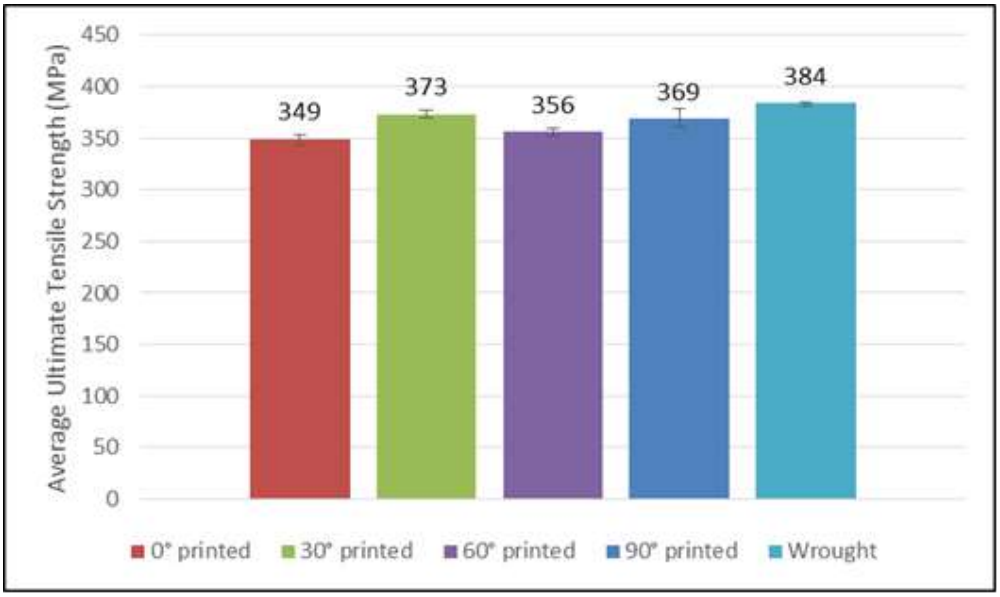

Fig. 5 Variation of UTS with specimen build orientation

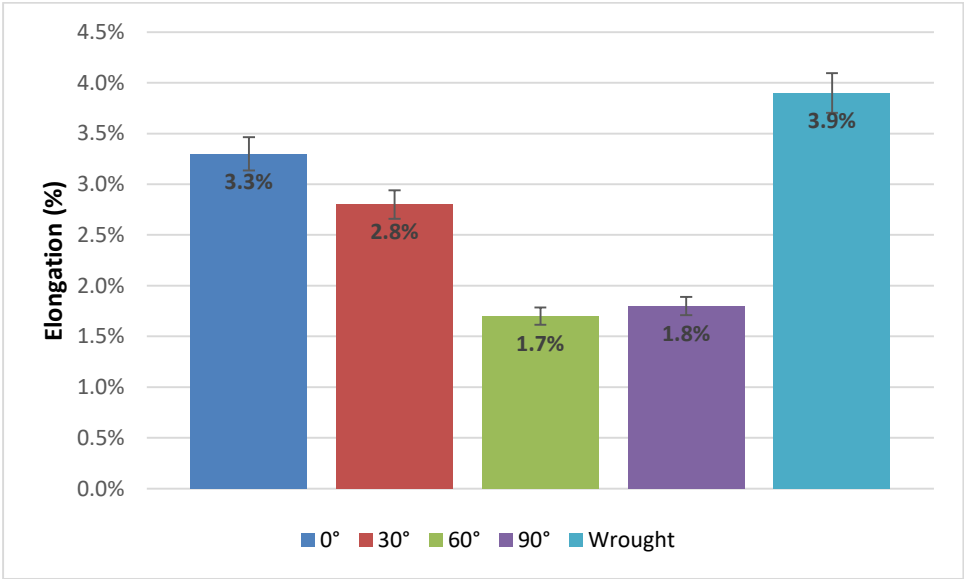

Fig. 6 Percent elongation as a function of specimen build angle

Effect of Specimen Build Angle on Ultimate Tensile Strength

Average UTS variation with specimen orientation is presented in Figure 5. As in the case of elastic modulus, ultimate tensile strength also was on par with that of the wrought samples with almost no effect on specimen build angles.

Finally, Figure 6 presents the specimen's average elongation at failure. The lower % elongation of LAM samples is attributed to their very fine microstructures in comparison to that of a wrought alloy. The decreasing trend within the LAM specimens may be attributed to orientation, due in part to the LAM heterogeneous microstructure.

Microstructure analysis

Figure 7 and Figure 8 demonstrate the microstructures of wrought and LAM processed Al alloy samples. These microstructures are distinctly different as they show Al-Si-Mg precipitates and melt pool network structure for the wrought and the 3D-printed ones, respectively.

Figure 7 demonstrates cross section of laser scan tracks or melt pools of different laser scanned layers including the overlapping of melt pools. The dimensions of the melt pools depend on the laser power and hatching distance selected during SLM process. These microstructures appear very similar to that of weld fillets. It reveals a fine crystalline structure formed due to rapid solidification of thin layers built upon previously solidified layers [25]. Void/porosity is clearly visible on these microstructures. It is evident that the additive manufactured aluminium alloy has a heterogeneous microstructure as opposed to that of a homogeneous structure of the wrought alloy.

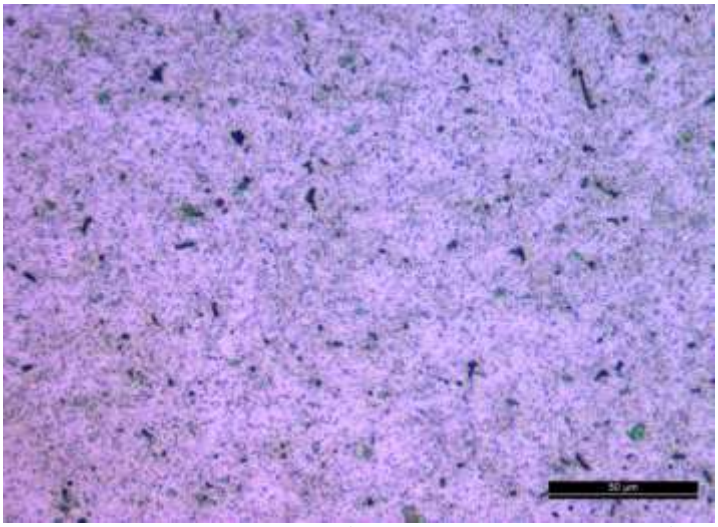

Fig. 7 Al-Si-Mg precipitates (appear as the black features) in an aluminium matrix of a wrought alloy

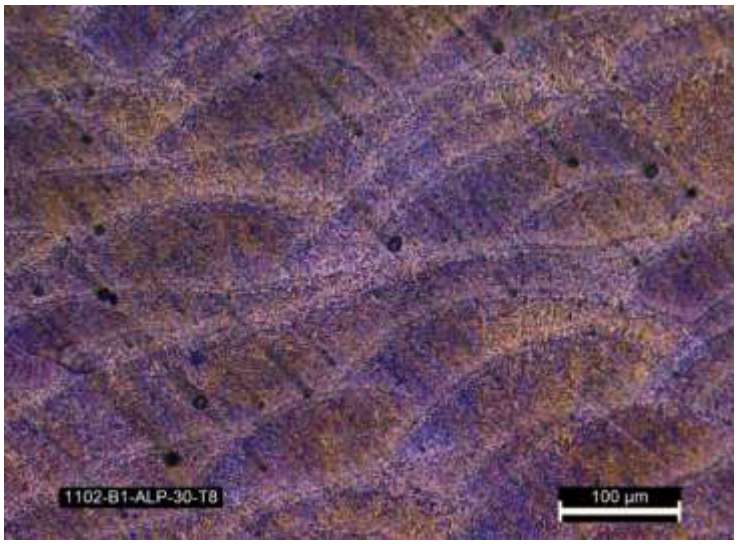

Fig. 8 LAM processed Al alloy demonstrating melt pool boundaries (ripples) and porosity defects (black features)

Fracture modes

Figures 9 and 10 reveal the fracture surface features of wrought and LAM processed aluminium alloys, respectively. Both wrought and LAM processed samples showed predominantly a ductile type fracture consisting of characteristic features like voids, dimples and ductile ridges [23].

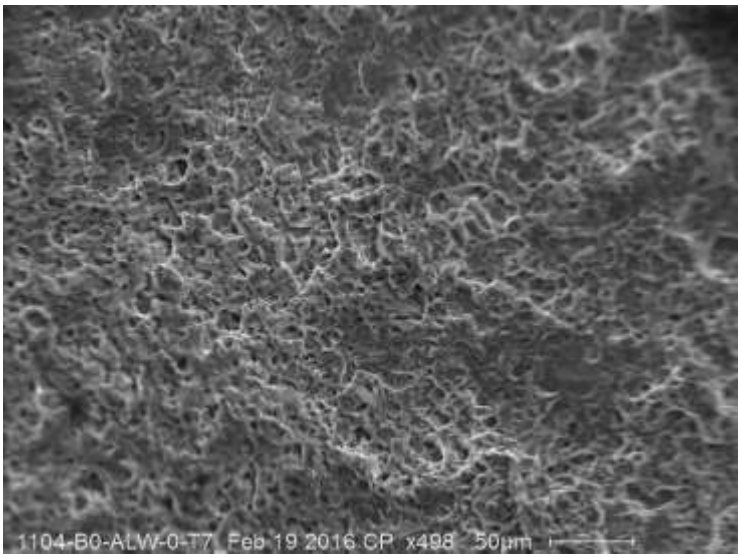

Fig. 9 Wrought tensile specimen demonstrating primarily ductile features

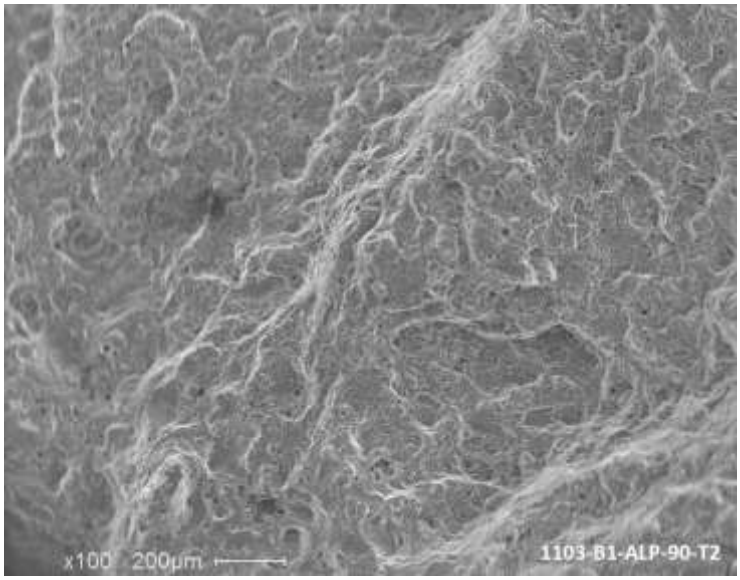

Fig. 10 LAM processed tensile specimen with dominant ductile fracture surface features

CONCLUSIONS

- The yield strength for the 0°, 30°, 60°, and 90° orientations in LAM samples are almost on par with each other but not with that of the wrought alloy.
- The ultimate tensile strength for the 0°, 30°, 60°, and 90° orientations in LAM samples are similar with that of the wrought alloy.
- The microstructure of additive manufactured AlSi10Mg alloy demonstrated heterogeneous structure. It contained overlapping weld pools with varying grain sizes due to the large temperature gradients from laser melting process versus predominantly homogeneous microstructure for the wrought specimen.
- The fracture surfaces of the additive manufactured (LAM) tensile specimens showed predominately ductile fracture characteristics for all build orientations similar to the wrought specimen features.

Acknowledgement

"Research was sponsored by the Army Research Laboratory and was accomplished under Cooperative Agreement Number W911NF-15-2-0020. The views and conclusions contained in this document are those of the authors and should not be interpreted as representing the official policies, either expressed or implied, of the Army Research Laboratory or the U.S. Government. The U.S. Government is authorized to reproduce and distribute reprints for Government purposes notwithstanding any copyright notation herein." The authors wish to thank Mr. Gary Wyss, Senior Scientist, CAMP, for SEM data analysis.

REFERENCES

[1] I Gibson, DW Rosen and B Stucker, *Additive Manufacturing Technologies*, First ed. Springer, **2010**.
[2] C Casavola, SL Campanelli and C Pappalettere, Preliminary Investigation on Distribution of Residual Stress Generated by the Selective Laser Melting Process, *Journal of Strain Analysis for Engineering Design*, **2009**, 44, 93–104.
[3] K Osakada and M Shiomi, Flexible Manufacturing of Metallic Products by Selective Laser Melting of Powder, *International Journal of Mach Tools Manufacturing*, **2006**, 46, 1188–1193.
[4] EO Olakanmi, RF Cochrane and KW Dalgarno, Densification Mechanism and Microstructural Evolution in Selective Laser Sintering of Al–12Si Powders, *Journal of Material Process Technology*, **2011**, 211, 113–21.
[5] C Yan, Y Shi, J Yang and J Liu, Preparation and Selective Laser Sintering of Nylon-12 Coated Metal Powders and Post Processing, *Journal of Material Process Technology*, **2009**, 209, 5785–92.
[6] A Liu, CK Chua and KF Leong, Properties of Test Coupons Fabricated by Selective Laser Melting, *Key Engineering Materials*, **2010**, 447-448, 780–784.
[7] U Tradowskya, J White, RM Ward, N Read, W Reimers and MM Attallah, Selective Laser Melting of $AlSi_{10}$mg: Influence of Post-Processing on the Microstructural and Tensile Properties Development, *Materials and Design*, **2016**, 105, 212–222.
[8] Thijs, K Kempen, JP Kruth and J Van Humbeeck, Fine-Structured Products with Controllable Texture by Selective Laser Melting of Pre-Alloyed Alsi10mg Powder, *Acta Materilia*, **2013**, 61 (5), 1809–1819.

[9] NT Aboulkhair, I Maskery, C Tuck, I Ashcroft and NM Everitt, On the Formation of AlSi10Mg Single Tracks and Layers in Selective Laser Melting: Microstructure and Nano-Mechanical Properties, *Journal of Materials Processing Technology*, **2016**, 230, 88–98.
[10] AK Gupta, DJ Lloyd and SA Court, Precipitation Hardening in Al–Mg–Si alloys with and Without Excess Si, *Materials Science and Engineering*, **2001**, A316, 11-17.
[11] L Thijs, K Kempen, JP Kruth and JV Humbeeck, Fine-Structured Aluminium Products with Controllable Texture by Selective Laser Melting of Pre-Alloyed Alsi10mg Powder, *Acta Materilia*, **2013**, 61, 1809–1819.
[12] K Kempen, L Thijs, JV Humbeeck and JP Kruth, Mechanical Properties of AlSi10Mg Produced by Selective Laser Melting, *Physics Procedia*, **2012**, 39, 439–446.
[13] E Brandl, U Heckenberger, V Holzinger and D Buchbinder, Additive Manufactured AlSi10mg Samples Using Selective Laser Melting (SLM): Microstructure High Cycle Fatigue and Fracture Behavior, *Materials & Design***, 2012**, 34, 159–169.
[14] EO Olakanmi, Selective Laser Sintering/Melting (SLS/SLM) of Pure Al, Al–Mg, and Al–Si Powders: Effect of Processing Conditions and Powder Properties, *Journal of Materials Processing Technology*, **2013,** 213, 1387– 1405.
[15] E Louvis, P Fox and CJ Sutcliffe, Selective Laser Melting of Aluminium Components, *Journal of Materials Processing Technology*, **2011**, 211, 275–284.
[16] EO Olakanmi, Direct Selective Laser Sintering of Aluminium Alloy Powders, *Institute for Materials Research*, Leeds, University of Leeds PhD, **2008**, 378.
[17] EO Olakanmi, RF Cochrane and KW Dalgarno, Densification Mechanism and Microstructural Evolution in Selective Laser Sintering of Al-12Si Powders, *Journal of Materials Processing Technology*, **2011**, 211 (1), 113–121.
[18] A Amirzadeh, M Raessi and S Chandra, Producing molten metal droplets smaller than the nozzle diameter using a pneumatic drop-on-demand generator, *Experimental Thermal and Fluid Science*, **2013**, 47, 26–33.
[19] EJ Vega, AM Gañán-Calvo, JM Montanero, MG Cabezas and MA Herrera, A Novel Technique ~~For~~for Producing Metallic Microjets and Microdrops *Microfluidics and Nanofluidics*, **2012**, 14, 101–111.
[20] Y Chao, L Qi, Y Xiao, J Luo and J Zhou, Manufacturing of Micro Thin-Walled Metal Parts by Micro-Droplet Deposition, *Journal of Materials Processing Technology*, **2012**, 212, 484–491.
[21] Y Chao, L Qi, H Zuo, J Luo, X Hou and H Li, Remelting and Bonding of Deposited Aluminium Alloy Droplets Under Different Droplet and Substrate Temperatures in Metal Droplet Deposition Manufacture, *International Journal of Machine Tools and Manufacture*, **2013**, 69, 38–47.
[22] M Fang, S Chandra and CB Park, Heat Transfer During Deposition of Molten Aluminium Alloy Droplets to Build Vertical Columns, *Journal of Heat Transfer*, 131, **2009**, 112101.
[23] Hansong Zuo, Hejun Li, Lehua Qi and Songyi Zhong, Influence of Interfacial Bonding between Metal Droplets on Tensile Properties of 7075 Aluminium Billets by Additive Manufacturing Technique, *Journal of Materials Science & Technology*, **2016**, 32, 485–488.
[24] KV Sudhakar, Penn Rawn, Bryce Abstetar, Ronda Coguill and Bruce Madigan, Additive Manufacturing of Stainless Steel: Processing, *Microstructure and Material Properties*, Salt Lake City, Utah, **2016**.
[25] TM Mower and MJ Long, Mechanical Behavior of Additive Manufactured, Powder-Bed Laser-Fused Materials, *Materials Science & Engineering A*, **2016**, 651, 198-213.